Journal of Biomedical Optics

BiomedicalOptics.SPIEDigitalLibrary.org

Validation of a method to measure light distortion surrounding a source of glare

Helena Ferreira-Neves
Rute Macedo-de-Araújo
Laura Rico-del-Viejo
Ana C. da-Silva
António Queirós
José M. González-Méijome

SPIE.

Validation of a method to measure light distortion surrounding a source of glare

Helena Ferreira-Neves, Rute Macedo-de-Araújo, Laura Rico-del-Viejo, Ana C. da-Silva, António Queirós, and José M. González-Méijome*
University of Minho, School of Science, Clinical and Experimental Optometry Research Lab, Centre of Physics, Gualtar, Braga 4710-057, Portugal

Abstract. Our objective was to validate a new device dedicated to measure the light disturbances surrounding bright sources of light under different sources of potential variability. Twenty subjects were involved in the study. Light distortion was measured using an experimental prototype (light distortion analyzer, CEORLab, University of Minho, Portugal) comprising twenty-four LED arrays panel at 2 m. Sources of variability included: intrasession and intersession repeated measures, pupil size (3 versus 6 mm), defocus (+0.50) correction for the working distance, angular resolution (15 deg versus 30 deg), temporal stimuli presentation, and pupil size. Size, shape, location, and irregularity parameters have been obtained. At a low speed of presentation of the stimuli, changes in angular resolution did not have an effect on the results of the parameters measured. Results did not change with pupil size. Intensity of the central glare source significantly influenced the outcomes. Examination time was reduced by 30% when a 30 deg angular resolution was explored instead of 15 deg. Measurements were fast and repeatable under the same experimental conditions. Size and shape parameters showed the highest consistency, whereas location and irregularity parameters showed lower consistency. The system was sensitive to changes in the intensity of the central glare source but not to pupil changes in this sample of healthy subjects. [DOI: 10.1117/1.JBO.20.7.075002]

Keywords: light distortion; glare; haloes; pupil size; validation.

Paper 150033R received Jan. 21, 2015; accepted for publication May 4, 2015; published online Jul. 6, 2015.

1 Introduction

Measurement of night vision disturbances (NVD) under dim light conditions has been a matter of interest for clinicians and researchers over the past decade. Although these disturbances were recognized much earlier, such phenomena have gained increased clinical relevance as a consequence of corneal refractive surgery[1–3] and implantation of intraocular lenses with complex optical designs.[4]

Under this generic concept of NVD, different entities are represented, including positive and negative dysphotopsia, halos, glare or starburst. Despite having different impacts on the subjective optical quality of the eye, different manifestations are not easily distinguishable or measured independently. For that reason, Klyce has suggested incorporating the term "light distortion" to include all of them.[5] Previous authors have suggested internal reflections in the intraocular prosthesis,[6] residual refractive error, higher order aberrations,[3] and ocular media opacities inducing light scattering[7] as potential etiological factors.

NVD are frequently self-reported by patients, but these are usually described as subjective complaints instead of objective and quantitative measures. With the increasing interest in intraocular surgery using different multifocal IOLs, there is a need to consistently measure the size and shape of such distortions. Beyond the use of subjective questionnaires and psychometric questionnaires, measurement of glare, haloes, and starbursts or light distortion as a comprehensive representation of those phenomena has been conducted with different methodologies.[7] Some of these methods are devoted to measuring the intraocular scattering, while others intend to measure the light distortion surrounding a bright spot of light against a dark background. This last approach can be done by using digital displays to project detection stimuli around sources of glare[8] or using methods to recognize letters or the orientation of characters surrounding a bright glare source.[9,10] The characteristics of the glare and detection sources were frequently not fully disclosed and the number of directions explored varied considerably between devices. Most of them reported only the size of the disturbance without specific reference to its position, shape or regularity.

Villa et al.[3] evaluated the light distortion by presenting peripheral stimuli using a computer-based facility to detect the size of the light distortion surrounding a bright light emitting diode (LED) by presenting white stimuli in a computer video display unit. Anera et al.[11] used the same device to evaluate the outcomes of a customized ablation compared with a standard algorithm for corneal refractive surgery. Later on, a fully computerized version of this device was used to evaluate the effect of optical opacities.[12] Sheppard et al.[10] used custom software to radially present random letters toward a central source of glare until the patients could not recognize the letters. They evaluated size of the light distortion surrounding a central source of glare in patients implanted with different multifocal IOLs. More recently, Puell et al.[9] investigated the size of the halo in the general population using a commercial vision monitoring device. This device measures the ability to recognize letters in three semimeridians around a source of glare at 2.5 m.

*Address all correspondence to: José M. González-Méijome, E-mail: jgmeijome@fisica.uminho.pt

1083-3668/2015/$25.00 © 2015 SPIE

A recent development of these systems was the Rostock Glare Perimeter developed by Meikies et al.[8] that uses peripheral stimuli presented from a digital projector system to a wall or screen at 3.3 m from the patient.

We have developed a device to measure the light distortion under more realistic and consistent conditions, using hardware with physical LEDs instead of projected light spots[12] for the generation of the light distortion as well as for the detection of the peripheral stimuli. This allows us to overcome some of the limitations of previous methods. By using point sources instead of letters, we aim to avoid the problem that the outcomes of the test are limited simply because of reading (or acuity) limitations; using a detection rather than resolution stimuli can also avoid the delay in response, increase the speed of the test, avoid loss of attention, and be clinically applicable in elderly patients. Being a physical device instead of software running on a computer screen also ensures that the experimental conditions in different settings can be comparable. The luminance that can be achieved with this system ranges from 0 to 3000 cd/m^2 for the central stimuli and 0 to 6 cd/m^2 for the peripheral stimuli.[13] This system provides different metrics of size, shape, location, and regularity offering more comprehensive information about the actual disturbance.

This feature might be useful in order to differentiate between the disturbances originated by different optical devices even when their size might be the same; this might be a clear advantage in asymmetric and/or decentered optical designs. Other methods measure the light distortion only in one direction and then consider that the same size is affected in all directions of the patient's field of view.[4,8,9]

With the present method, we aim to evaluate the consistency of the light distortion analyzer (LDA) device under different sources of variability including spatial, temporal, and clinical routine issues (intersession, intrasession, pupil size). It is also the aim of this work to estimate the duration of the examination under different conditions.

2 Methods

2.1 *Sample*

Twenty healthy volunteers (12 females, 8 males) participated in the study. All subjects had normal ocular and general health, with ages ranging from 23 to 37 yr (26.4 ± 6.1 yr). Inclusion criteria required that the subjects had no complaints of dry eye, do not wear contact lenses and present a tear-film break-up time of at least 10 s measured prior to enrollment in the study.

All subjects were submitted to a full optometric examination including: objective and subjective refraction using an end-point criterion of maximum plus for the best visual acuity; pupil diameter measurement (NeurOptics® VIP™-200, California) and whole eye wavefront aberrometry using a Harmann-Shack aberrometer (IRX3, Imagine Eyes, Orsay, France).

Following the tenets of the Declaration of Helsinki, all subjects signed an informed consent after the nature and possible consequences of the study had been explained.

2.2 *Procedure*

Light distortion measurements were done using the LDA developed at the CEORLab, University of Minho, Portugal. This is an experimental prototype device comprising an electronic black board with a central light source (LED) with a high-intensity power output surrounded by 240 small LED sources with smaller intensity power outputs. The central LED is responsible for creating the glare condition while the surrounding LEDs are used as threshold discriminators at different positions and angular distances in the visual field.[13] The peripheral LED's are distributed in twenty-four semimeridians with a minimum angular separation of 15 deg. Figure 1 represents the layout arrangement of the central white LED and the surrounding smaller white LEDs. The central LED was a commercially available white LED from Agilent Technologies (ref. HLMP-CW47-RU000 from Agilent Technologies, Inc., Berkshire, United Kingdom); the surrounding LEDs were commercially available white LEDs from Avago Technologies (ref. HSMW-CL25 from Avago Technologies, San Jose, California). The calibration and radiometric description of the central and peripheral LEDs that constitute the device have been done and have been proven successful for use in visual assessments.[13] The physical display (electronic board) is connected to a control central control device (PC computer) and the subject being evaluated provides feedback to the system through a remote response device (PC mouse). Peripheral stimuli are presented around the central source of light using different sequences at random times from 250 to 750 ms and the different semimeridians are explored in random order. When the subject sees the peripheral stimulus, he/she presses the mouse control button and the system presents the next semi meridian. Three evaluations are performed in each semi meridian before the instrument calculates the mean limit of the light distortion. If the standard deviation (SD) of the three measurements in each semimeridian is above 20% of the mean value, the device automatically repeats the measurements in those semi meridians until it reaches values of SD below 20% of the mean.

Only the information of the right eye is presented in order to avoid duplication of the sample considering the related nature of the information obtained from both eyes of the same subjects.

Figure 2 shows the structure of the protocol of the study that was divided into two different phases.

In the first phase of the study, the measurements were obtained using different examination strategies (in-out, out-in, subjective), different angular separations (15 deg /24 radial directions; 30 deg /12 radial directions), two different velocities of peripheral stimuli presentation times (ON-OFF intervals of 250 to 750 ms) and the different semimeridians were explored in random order. "In-out" refers to the strategy where the radial

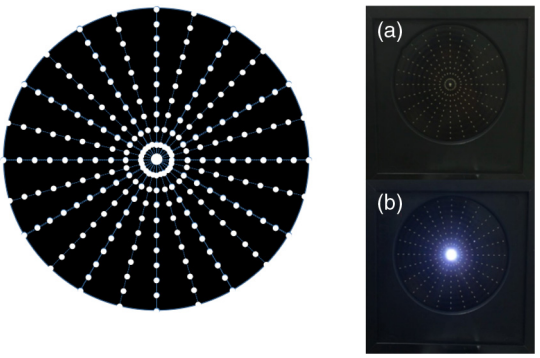

Fig. 1 Illustration of the distribution of one central source of light and 240 peripheral stimuli; central and peripheral stimulus at 15 deg, semi meridians are turned-on. Device with the central LED light turned off (A) and turned on at minimum intensity (B).

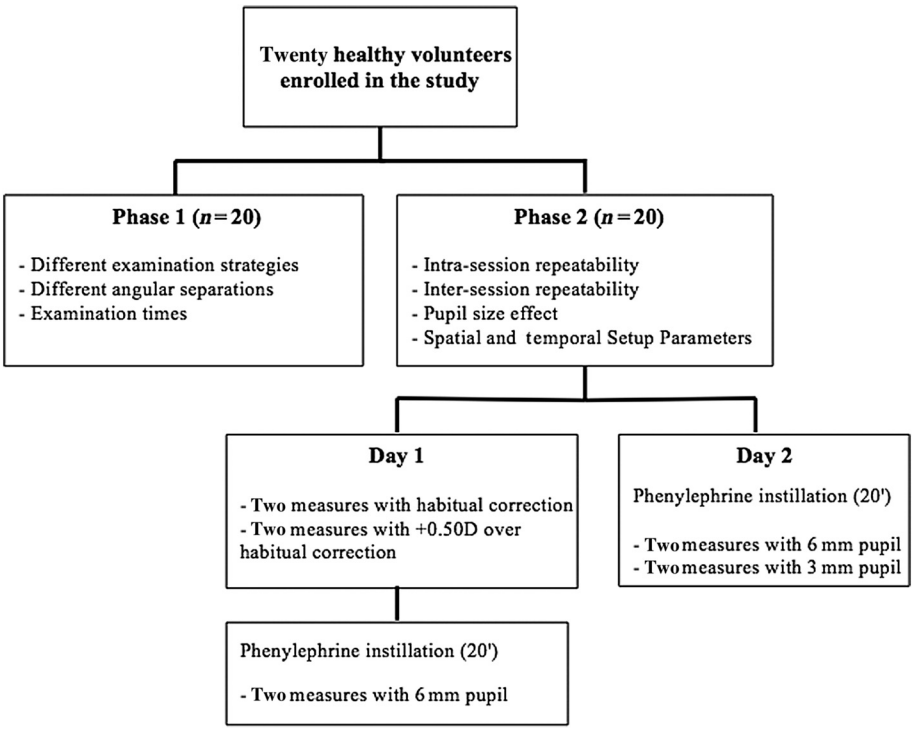

Fig. 2 Structure of the protocol of the study.

LEDs turn-on sequentially from the center to the periphery until detection; "out-in" refers to the strategy where LEDs turn-on from the periphery to the center until not detected; "subjective" refers to the exam where the subject moves the light along a radial direction until the edge of the distortion is reached. The radial directions are randomly evaluated in all exam strategies. Examination time was recorded for later comparison between the different testing strategies. The speed of presentation of the stimuli (ON–OFF times) was random from 250 to 750 ms in order to avoid false responses from the subject.

In the second phase of the study two different measurements were recorded in two different sessions using an "In-out" strategy with three different intensities for the central LED (minimum 1% to 30 cd/m^2, medium 50% to 1500 cd/m^2, maximum 100% to 3000 cd/m^2). First, measurements with natural pupil were done with and without a +0.50 D lens to compensate the vergence induced by the fixation target placed at a 2 m distance.

After the measurements with natural pupil, the patients were dilated with 1% phenylephrine (Davinefrina, DAVI II, Portugal) and, after 30 min, the measurements were repeated with an artificial pupil of 6 mm in the first session and 3 and 6 mm in the second session.

All measurements were performed with the best distance correction from a distance of 2 m from the display, with the room in total darkness while the patient was seated and stabilized using a chin rest with the eyes at the level of the central source of light. All data obtained and processed for statistical analysis is the result of three repeated valid measures obtained by the instrument and averaged.

The system derives different metrics from each examination. They are summarized below:

- Distortion area (DA): is calculated as the sum of the areas of all triangles (or sectors) formed between each pair of semimeridians under analysis, in mm^2.
- Light distortion index (LDI): percentage of the total tested area that is not visible because of impairment by the light distortion phenomena. It is calculated as the ratio of the area missed by the subject and the total area explored and is expressed as a percentage (%). Higher values of LDI are interpreted as the lower ability to discriminate surrounding small stimuli that are by the central source of light.
- Best fit circle radius (BFC_{Rad}): as the DA is formed by an irregular polygonal shape that results from the linking of the outer limits of the distortion along each semimeridian, a circle that best fits this shape is derived whose radius is equal to the average length of the distortion along each semimeridian under evaluation (Length) expressed in mm.
- Best fit circle center coordinates (X_{Coord} and Y_{Coord}): defined as Cartesian coordinates (x, y) in mm from the center of the display.
- Orientation of best fit circle center (BFC_{Orient}): angle of BFC center from the origin of coordinates (0,0), which is the center of the display. Expressed in deg.
- DA irregularity (BFC_{Irreg}): sum of the deviations between the actual DA and the BFC outer perimeter along all the semimeridians tested. It is a sum of positive and negative values as the limit of the distortion is in or out of the BFC perimeter and is expressed in mm.
- SD of the BFC irregularity ($BFC_{IrregSD}$): sum of the differences squared and divided by the number of semimeridians tested (n). Higher values of $BFC_{IrregSD}$ means a more irregular distortion. Expressed in mm.

2.3 *Statistical Analysis*

Statistical analysis has been conducted using SPSS v21.0 (IBM Inc., Illinois). Normality was checked by the Shapiro-Wilk test

Table 1 Medians and interquartile range (IQR) for the data from phase 1 of the study.

LDA parameters			DA (mm^2)	LDI (%)	BFC_{Rad} (mm)	X_{Coord} (mm)	Y_{Coord} (mm)	BFC_{Orient} (deg)	BFC_{Irreg} (mm)	$BFC_{IrregSD}$ (mm)
Habitual correction (natural pupil)										
Minimum intensity	Measure 1	Median	544.00	2.71	13.30	0.00	0.24	166.10	0.40	4.18
		IQR	728.00	3.63	8.00	0.33	0.46	120.00	0.75	1.13
	Measure 2	Median	704.00	3.50	15.30	−0.42	0.33	150.00	0.28	3.56
		IQR	576.00	2.87	6.30	0.91	1.05	97.50	0.24	0.94
Medium intensity	Measure 1	Median	768.00	3.82	16.00	0.00	−0.33	230.10	0.09	3.30
		IQR	312.00	1.56	2.65	1.15	0.46	105.00	0.22	0.84
	Measure 2	Median	768.00	3.82	16.00	0.00	0.00	180.00	0.23	2.15
		IQR	448.00	2.23	4.05	0.33	0.63	105.00	0.32	2.58
Maximum intensity	Measure 1	Median	992.00	4.93	18.00	−0.58	−0.33	210.00	0.40	3.11
		IQR	1024.00	5.09	7.40	0.90	0.76	38.80	0.28	1.59
	Measure 2	Median	1280.00	6.37	20.70	0.33	0.00	180.00	0.15	3.93
		IQR	1056.00	5.26	7.35	0.41	1.05	224.32	0.34	1.38
Habitual correction +0.50 D										
Minimum intensity	Measure 1	Median	768.00	3.82	16.00	−0.42	0.24	150.00	0.38	3.51
		IQR	600.00	2.99	6.05	0.70	0.79	64.40	0.23	1.55
	Measure 2	Median	768.00	3.82	16.00	0.00	0.09	150.00	0.23	3.08
		IQR	464.00	2.31	5.35	0.84	0.29	160.61	0.43	2.14
Medium intensity	Measure 1	Median	1184.00	5.89	20.00	0.00	0.00	180.00	0.10	4.15
		IQR	832.00	4.14	6.30	0.50	1.05	129.82	0.40	3.11
	Measure 2	Median	1024.00	5.09	18.70	−0.33	0.00	180.00	0.32	2.74
		IQR	792.00	4.04	6.70	0.79	1.13	99.15	0.19	1.35
Maximum intensity	Measure 1	Median	1712.00	8.51	24.00	0.00	0.24	165.00	0.27	4.91
		IQR	1816.00	9.03	11.35	0.96	1.74	124.95	0.63	0.59
	Measure 2	Median	1744.00	8.67	24.00	−0.33	−0.42	204.90	0.42	4.07
		IQR	1504.00	7.48	10.00	0.54	1.82	152.55	0.19	0.58
Pupil 6 mm Day1										
Minimum intensity	Measure 1	Median	384.00	1.91	11.30	0.00	−0.24	270.00	0.69	3.93
		IQR	1024.00	5.10	10.70	0.79	1.99	131.46	0.48	1.75
	Measure 2	Median	783.00	3.90	16.00	−0.09	−0.09	195.00	0.40	3.72
		IQR	680.00	3.38	6.65	0.67	1.20	111.32	0.41	1.07
Medium intensity	Measure 1	Median	976.00	4.85	18.00	0.09	−0.33	195.00	0.45	3.91
		IQR	1544.00	7.68	11.05	1.03	0.92	103.98	0.22	0.97
	Measure 2	Median	1120.00	5.57	19.30	0.24	−1.24	249.90	0.38	4.03
		IQR	1456.00	7.25	10.70	0.96	1.58	112.50	0.55	1.41

Table 1 (*Continued*).

LDA parameters			DA (mm^2)	LDI (%)	BFC_{Rad} (mm)	X_{Coord} (mm)	Y_{Coord} (mm)	BFC_{Orient} (deg)	BFC_{Irreg} (mm)	$BFC_{IrregSD}$ (mm)
Maximum intensity	Measure 1	Median	1280.00	6.37	20.70	−0.24	−0.58	255.00	0.46	4.83
		IQR	1912.00	9.51	12.35	1.50	2.11	162.73	0.98	3.95
	Measure 2	Median	1536.00	7.64	22.70	−0.15	−1.15	263.79	0.21	4.31
		IQR	1896.00	9.43	11.65	0.49	1.46	95.19	0.20	1.52
Pupil 6-mm Day 2										
Minimum intensity	Measure 1	Median	704.00	3.50	15.30	0.09	−0.33	246.21	0.48	3.96
		IQR	1016.00	5.06	18.30	0.46	0.17	268.29	1.14	5.52
	Measure 2	Median	592.00	2.94	14.00	0.33	−1.49	241.94	1.09	3.53
		IQR	536.00	2.66	6.35	1.87	1.75	80.74	0.62	2.65
Medium intensity	Measure 1	Median	912.00	4.54	17.30	−0.91	−1.24	255.00	0.71	3.57
		IQR	1352.00	6.73	10.70	0.79	1.79	62.00	0.59	1.36
	Measure 2	Median	1152.00	5.73	19.30	−0.91	−0.58	240.00	0.50	4.15
		IQR	1296.00	6.45	9.65	1.70	1.75	137.04	0.93	5.26
Maximum intensity	Measure 1	Median	1696.00	8.44	24.00	−0.91	0.67	142.86	0.50	4.21
		IQR	1520.00	7.56	10.00	1.20	3.40	142.50	0.59	10.56
	Measure 2	Median	1376.00	6.84	21.30	0.00	0.00	180.00	0.48	3.38
		IQR	1664.00	8.28	11.65	0.38	2.65	129.56	0.50	3.78
Pupil 3-mm Day 2										
Minimum intensity	Measure 1	Median	704.00	3.50	16.00	0.07	−0.24	210.00	0.62	5.90
		IQR	1024.00	5.09	10.00	1.91	1.58	182.55	0.68	1.82
	Measure 2	Median	528.00	2.63	13.30	0.00	−0.49	265.89	0.44	5.10
		IQR	664.00	3.30	7.65	0.59	0.51	51.95	0.66	2.60
Medium intensity	Measure 1	Median	1248.00	6.21	20.70	−0.33	0.00	172.48	0.39	5.19
		IQR	1408.00	7.00	11.70	1.58	0.66	142.50	0.24	2.90
	Measure 2	Median	960.00	4.77	18.00	−0.67	0.33	150.00	0.50	3.19
		IQR	1096.00	5.45	10.30	0.79	1.65	84.39	0.70	7.60
Maximum intensity	Measure 1	Median	1840.00	9.15	24.70	0.91	0.24	79.49	0.68	4.51
		IQR	1696.00	8.43	12.65	1.78	2.91	186.34	0.83	7.54
	Measure 2	Median	1728.00	8.59	24.00	−0.42	0.58	120.00	0.21	3.84
		IQR	1584.00	7.88	12.65	0.37	2.00	130.30	0.45	4.51

and due to the nature of the data, nonparametric statistics were applied. For the multiple comparisons, a Friedman test with posthoc correction has been applied and Wilcoxon signed ranks for pair-wise comparison. The level of statistical significance has been set at $p < 0.05$. Spearman rank correlation coefficients (r) were calculated considering that a strong correlation was classified as a coefficient greater than 0.8, moderately strong within the range of 0.5 to 0.8, fair within the range of 0.3 to 0.5, and poor at less than 0.3.[14]

3 Results

Average manifest spherical and cylindrical subjective refractions were $+0.43 \pm 0.30$ D and -0.12 ± 0.17 D, respectively. Average maximum round pupil in mesopic conditions was

Table 2 Statistical comparison (p) and correlation analysis (r) of the light distortion parameters measured with patient's habitual correction and using a +0.50 D lens over the habitual correction for compensating the vergence induced by the target placed at 2 m from the subject. Results are shown for an "in-out" strategy with three different intensities for the central LED (minimum 1% to 30 cd/m^2; medium 50% to 1500 cd/m^2; and maximum 100% to 3000 cd/m^2).

	Central LED at minimum intensity		Central LED at medium intensity		Central LED at maximum intensity	
+0.50 D Over habitual correction	p	r	p	r	p	r
DA (mm^2)	0.528	**0.937+**	0.345	**0.847**[a]	0.063	0.721
LDI (%)	0.528	**0.937+**	0.345	**0.847**[a]	0.063	0.721
BFC_{Rad} (mm)	0.674	**0.927+**	0.207	**0.847**[a]	0.063	0.721
X_{Coord} (mm)	0.344	0.127	0.116	0.579	**0.018**	0.615
Y_{Coord} (mm)	0.686	0.200	0.799	0.018	0.932	0.345
BFC_{Orient} (deg)	0.080	0.664	0.553	−0.291	0.612	0.487
BFC_{Irreg} (mm)	0.735	**−0.090**	0.345	0.108	0.236	−0.286
$BFC_{IrregSD}$ (mm)	0.398	0.198	0.600	−0.327	0.612	−0.321

Note: p: Wilcoxon signed ranks test; r: Spearman's correlation; bold means statistically significant values.
[a]Correlation is significant at the 0.01 level; +correlation is significant at the 0.05 level.

5.10 ± 0.11 mm under nondilated conditions and 7.10 ± 0.21 mm after phenylephrine instillation. The average 4th order spherical aberrations (SA) for a 6 and 3-mm pupil were 0.09 ± 0.06 μm and 0.01 ± 0.02 μm and total high order aberrations (HOAs) root mean square were 0.38 ± 0.15 μm and 0.09 ± 0.03 μm, respectively. LDA parameters did not follow normal distribution according to the Shapiro-Wilk test. Therefore, nonparametric statistics were conducted. Table 1 shows the median and interquartile range for the data gathered in phase 1 of the study.

Results are presented in the following subsections for the following factors: (a) compensation of the vergence at the examination distance with three different intensities of the central source; (b) intrasession agreement for the natural pupil size, 6 mm in session 1 and session 2 and 3 mm artificial pupils with three different intensities of the central source; (c) intersession

Table 3 Statistical comparison (p value) and correlation analysis (r) of the light distortion parameters between two consecutive measurements in the same condition (for pupil sizes of 3 and 6 mm). Results are shown for an "in-out" strategy with three different intensities for the central LED (minimum 1% to 30 cd/m^2; medium 50% to 1500 cd/m^2; and maximum 100% to 3000 cd/m^2).

	Central LED at Minimum Intensity				Central LED at Medium Intensity				Central LED at Maximum Intensity			
	Pupil 6 mm		Pupil 3 mm		Pupil 6 mm		Pupil 3 mm		Pupil 6 mm		Pupil 3 mm	
Intrasession	p	r	p	r	p	r	p	r	p	r	p	r
DA (mm^2)	0.866	0.955[a]	0.672	0.964[a]	0.735	0.821[b]	0.833	0.786[b]	0.735	0.969[a]	0.672	0.999[a]
LDI (%)	0.735	0.955[a]	0.735	0.964[a]	0.735	0.821[b]	0.833	0.786[b]	0.735	0.821[b]	0.735	1.000[a]
BFC_{Rad} (mm)	0.734	0.955[a]	0.746	0.964[a]	0.866	0.811[b]	0.833	0.775[b]	0.734	0.957[a]	0.746	0.995[a]
X_{Coord} (mm)	0.735	0.414	0.176	−0.414	0.917	−0.429	0.237	−0.109	0.735	−0.487	0.176	−0.162
Y_{Coord} (mm)	0.310	−0.321	0.553	−0.679	0.398	0.180	0.249	0.250	0.310	0.679	0.553	0.536
BFC_{Orient} (deg)	0.128	−0.450	0.237	0.107	0.799	0.180	0.866	0.571	0.128	0.464	0.237	−0.09
BFC_{Irreg} (mm)	0.204	0.393	**0.018**	0.036	0.866	−0.500	0.236	0.018	0.204	−0.273	**0.018**	0.250
$BFC_{IrregSD}$ (mm)	0.063	0.429	0.091	0.571	0.310	0.714	0.398	0.714	0.063	0.607	0.091	0.714

Note: p: Wilcoxon signed ranks test; r: Spearman's correlation; and bold means statistically significant values.
[a]Correlation is significant at the 0.05 level.
[b]Correlation is significant at the 0.01 level.

Table 4 Statistical comparison (p value) and correlation analysis (r) of the light distortion parameters measured in two different sessions (days) for a pupil size of 6 mm. Results are shown for an "in-out" strategy with three different intensities for the central LED (minimum 1% to 30 cd/m^2; medium 50% to 1500 cd/m^2; and maximum 100% to 3000 cd/m^2).

	Central LED at Minimum Intensity		Central LED at Medium Intensity		Central LED at Maximum Intensity	
Intersession (for 6 mm pupil)	p	r	p	r	p	r
DA (mm^2)	0.866	**0.793**[a]	0.499	**0.857**[a]	0.735	**0.990**[b]
LDI (%)	0.866	**0.793**[a]	0.499	**0.857**[a]	0.735	0.714
BFC_{Rad} (mm)	0.733	**0.793**[a]	0.400	**0.893**[b]	0.866	**0.773**[a]
X_{Coord} (mm)	1.000	−0.667	0.398	−0.143	0.916	0.704
Y_{Coord} (mm)	0.310	−0.491	0.752	−0.054	1.000	0.216
BFC_{Orient} (deg)	0.499	0.143	0.310	0.571	0.398	0.396
BFC_{Irreg} (mm)	**0.028**	**0.821**[a]	0.310	−0.393	0.128	−0.054
$BFC_{IrregSD}$ (mm)	0.176	0.179	0.237	0.464	0.612	0.250

Note: p: Wilcoxon signed ranks test; r: Spearman's correlation; and bold means statistically significant values.
[a]Correlation is significant at the 0.01 level.
[b]Correlation is significant at the 0.05 level.

agreement for the 6 mm pupil size in session 1 and session 2; (d) pupil size for 6 and 3 mm artificial pupil size; (e) intensity of the central source; (f) spatial and temporal setup parameters.

3.1 *Compensation of the Vergence Induced by the Fixation Target*

Table 2 shows the statistical comparison of the light distortion parameters measured with the patient's habitual correction and by placing a +0.50 D lens over the habitual correction for compensating the vergence induced by the fixation target (2 m). Results show that there were found no differences in terms of size (DA, LDI, and BFC_{Rad}), location (X and Y axis), and irregularity (BFC_{Irreg} and $BFC_{IrregSD}$) of the light distortion measured with different intensities of the central LED. The exception was the X coordinate of the BFC center with the maximum central LED intensity, in which the median value was significantly displaced toward negative values with the +0.50 D lens (0.33 mm versus −0.33 mm, $p = 0.018$). Correlations between the two measurements for all conditions were found to be strong ($r = 0.840$) for all the size parameters with the central LED light at minimum and medium intensities, and was moderately strong with the maximum intensity ($r = 0.721$).

3.2 *Intrasession*

Table 3 shows the statistical comparison of two consecutive measures for different conditions to study the intrasession repeatability. Results show that no differences were found in terms of size (DA, LDI, and BFC_{Rad}), location (X and Y axis), and irregularity (BFC_{Irreg} and $BFC_{IrregSD}$) of the light distortion measured in all of central LED intensities between the two measures in the same session. This is true for all parameters, except for the $BFC_{IrregSD}$ with a 3-mm pupil for minimum and maximum central LED intensities (both $p = 0.018$). Correlations between the two measurements for all conditions were found to be strong for the size parameters (DA, LDI, and BFC_{Rad}). Moderately strong correlations were found for the two pupil sizes in the $BFC_{IrregSD}$ parameter in all central LED light intensities except for the 6-mm pupil with the central LED light at minimum intensity ($r = 0.429$).

3.3 *Intersession*

Table 4 shows the statistical comparison of the light distortion parameters measured in two different sessions (days) for a pupil

Table 5 Statistical comparison (p value) and correlation analysis (r) of light distortion parameters measured for two different pupil sizes of 6 and 3 mm. Results are shown for an "in-out" strategy with three different intensities for the central LED (minimum 1% to 30 cd/m^2; medium 50% to 1500 cd/m^2; and maximum 100% to 3000 cd/m^2).

Pupil effect (6 mm versus 3 mm)	Central LED at minimum intensity	Central LED at medium intensity	Central LED at maximum intensity
DA (mm^2)	0.462	0.128	0.499
LDI (%)	0.462	0.128	0.499
BFC_{Rad} (mm)	0.528	0.176	0.553
X_{Coord} (mm)	0.528	0.498	0.352
Y_{Coord} (mm)	0.446	0.176	0.237
BFC_{Orient} (deg)	0.128	0.128	0.499
BFCIrreg (mm)	**0.046**	0.612	0.612
$BFC_{IrregSD}$ (mm)	0.612	0.735	0.176

Note: p: Wilcoxon signed ranks test and bold means statistically significant values.

Table 6 Statistical comparison of the effect of different central LED light intensities in light distortion measured with patient's natural pupil size, for pupil sizes of 6 and 3 mm. Results are shown for an "in-out" strategy with three different intensities for the central LED (*a*: minimum 1% to 30 cd/m^2; *b*: medium 50% to 1500 cd/m^2; and *c*: maximum 100% to 3000 cd/m^2).

Intensity effect		Minimum (a)–medium (b) intensity	Minimum (a)–Maximum (c) Intensity	Medium (b)–Maximum (c) Intensity
Natural pupil	DA (mm^2)	**0.027** (*b* > *a*)	**0.028** (*c* > *a*)	**0.028** (*c* > *b*)
	LDI (%)	**0.027** (*b* > *a*)	**0.028** (*c* > *a*)	**0.028** (*c* > *b*)
	BFC_{Rad} (mm)	**0.028** (*b* > *a*)	**0.028** (*c* > *a*)	**0.027** (*c* > *b*)
	X_{Coord} (mm)	0.599	0.249	**0.043** (*b* > *c*)
	Y_{Coord} (mm)	0.917	0.207	0.753
	BFC_{Orient} (deg)	0.115	0.893	0.753
	BFC_{Irreg} (mm)	0.176	0.108	0.600
	$BFC_{IrregSD}$ (mm)	0.237	0.310	0.075
Pupil 6 mm	DA (mm^2)	**0.018** (*b* > *a*)	**0.018** (*c* > *a*)	**0.028** (*c* > *b*)
	LDI (%)	**0.018** (*b* > *a*)	**0.018** (*c* > *a*)	**0.028** (*c* > *b*)
	BFC_{Rad} (mm)	**0.018** (*b* > *a*)	**0.018** (*c* > *a*)	**0.041** (*c* > *b*)
	X_{Coord} (mm)	0.310	0.933	0.445
	Y_{Coord} (mm)	1.000	0.735	0.933
	BFC_{Orient} (deg)	0.753	0.612	0.176
	BFC_{Irreg} (mm)	0.866	0.612	0.398
	$BFC_{IrregSD}$ (mm)	0.176	1.000	0.063
Pupil 3 mm	DA (mm^2)	**0.046** (*b* > *a*)	**0.028** (*c* > *a*)	**0.028** (*c* > *b*)
	LDI (%)	**0.046** (*b* > *a*)	**0.028** (*c* > *a*)	**0.028** (*c* > *b*)
	BFC_{Rad} (mm)	**0.046** (*b* > *a*)	**0.028** (*c* > *a*)	**0.027** (*c* > *b*)
	X_{Coord} (mm)	**0.018** (*b* < *a*)	0.063	0.31
	Y_{Coord} (mm)	0.063	0.398	0.753
	BFC_{Orient} (deg)	**0.018** (*b* < *a*)	**0.028** (*c* < *a*)	0.917
	BFC_{Irreg} (mm)	0.735	0.735	0.128
	$BFC_{IrregSD}$ (mm)	0.612	0.31	0.917

Note: *p*: Wilcoxon signed ranks test; bold means statistically significant values; *a*: median value with central LED at minimum intensity; *b*: median value with central LED at medium intensity; and *c*: median value with central LED at maximum intensity.

size of 6 mm. Results show that no differences were found in terms of size (DA, LDI, and BFC_{Rad}), location (X and Y axis), and irregularity (BFC_{Irreg} and $BFC_{IrregSD}$) of the NVD measured in all of central LED intensities, except for BFC_{Irreg} parameter with central LED at minimum intensity (medians: Day 1 = 0.69 mm, Day2: 0.48 mm; $p = 0.028$). Correlations between the two measurements were found to be moderately strong to strong ($r > 0.7$) for all the size parameters, being fair to poor in the location and regularity parameters, except for BFC_{Irreg} with the central LED light at minimum intensity ($r = 0.821$).

3.4 *Pupil Size*

Table 5 shows the statistical comparison of the light distortion parameters measured for pupil sizes of 6- and 3-mm. Results show that no differences were found in terms of size (DA, LDI, and BFC_{Rad}), location (X and Y axis), and irregularity (BFC_{Irreg} and $BFC_{IrregSD}$) of the NVD measured in all of central LED intensities, except for BFC_{Irreg} parameter with central LED at minimum intensity that was found to be lower with a 3-mm pupil (medians: 1.09 mm versus 0.44 mm, $p = 0.046$).

Table 7 Comparison between the different spatial and temporal setups that can be used to measure light distortion with the LDA.

	Subjective 30 deg	In-out 15 deg 15	In-out 15 deg 25	In-out 30 deg 15	In-out 30 deg 25
			DA (mm^2)		
Subjective 15 deg	**0.003**	0.952	0.054	0.501	0.751
Subjective 30 deg		0.240	**0.004**	0.378	0.070
In-out 15 deg 15			**0.001**	0.287	0.184
In-out 15 deg 25				**<0.001**	**0.001**
In-out 30 deg 15					**0.010**
			LDI (%)		
Subjective 15 deg	**0.012**	0.940	0.057	0.852	0.526
Subjective 30 deg		0.433	**0.008**	0.349	0.067
In-out 15 deg 15			**0.001**	0.852	**0.019**
In-out 15 deg 25				**<0.001**	0.048
In-out 30 deg 15					**0.009**
			BFC_{Rad} (mm)		
Subjective 15 deg	**0.010**	0.943	0.064	0.985	0.390
Subjective 30 deg		0.341	**0.007**	0.257	0.054
In-out 15 deg 15			**0.002**	0.985	**0.030**
In-out 15 deg 25				**<0.001**	**0.010**
In-out 30 deg 15					**0.008**
			BFC_{Irreg} (mm)		
Subjective 15	0.940	**0.001**	**<0.001**	**<0.001**	**<0.001**
Subjective 30		**0.004**	**0.001**	**0.003**	**0.001**
In out 15 deg 15			0.418	0.503	**0.027**
In-out 15 deg 25				0.699	0.409
In-out 30 deg 15					0.119
			$BFC_{IrregSD}$ (mm)		
Subjective 15 deg	0.191	**<0.001**	**<0.001**	**<0.001**	**<0.001**
Subjective 30 deg		0.065	**0.004**	**0.003**	**0.002**
In-out 15 deg 15			0.397	0.097	**0.007**
In-out 15 deg 25				0.434	0.113
In-out 30 deg 15					0.458

Note: *p*: Wilcoxon signed ranks test and bold means statistically significant values.

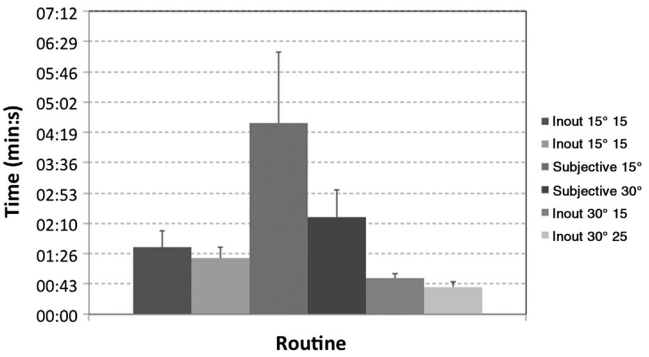

Fig. 3 Time spent doing the examination of light distortion with the different routine settings. Each measurement is the result of the average of three repetitions along each radial direction with a standard deviation below 20% the value recorded.

3.5 *Central Source Intensity*

Table 6 shows the effect of the different central LED light intensities on light distortion for natural, 6- and 3-mm pupil sizes. It can be seen that a significant increment of the size of the light distortion along with an increment of the central LED light intensity ($a < b < c$) was found. The location and shape parameters were more independent of the central LED light intensity despite the differences found for the X coordinate with pupil ($X_{medium} = 0.00$ mm, $X_{maximum} = 0.33$ mm; $p = 0.043$) and with a 3-mm pupil ($X_{minimum} = 0.00$ mm, $X_{maximum} = 0.42$ mm; $p = 0.018$).

3.6 *Spatial and Temporal Setup Parameters*

Table 7 shows the comparison between the different spatial and temporal setups that can be used to measure light distortion with the LDA. Changing the angular separation in the in-out exam but maintaining a low velocity of the peripheral stimulus (15) did not change the results of light distortion in terms of size, location, and regularity parameters. Notwithstanding, the same did not happen for the higher velocity of the peripheral stimulus (25), in which differences in the area of the distortion (DA 15 deg $= 0.67 \pm 0.11$ mm^2, DA 30 deg $= 0.61 \pm 0.08$ mm^2, $p = 0.001$) and radius of the BFC (BFC_{Rad} 15 deg $= 16.22 \pm 1.20$ mm^2, BFC_{Rad} 30 deg $= 15.70 \pm 1.02$ mm^2, $p = 0.010$) were found. On the contrary, when the angular separation was maintained and the velocity of the peripheral stimulus was changed, the light distortion was slightly greater with a higher velocity of the peripheral stimulus in terms of size (all $p < 0.05$), but regularity parameters were maintained for both angular separations (all $p > 0.05$). The subjective exam was found to be significantly altered when done with the two different angular separations in terms of the size of light distortion, being slightly smaller with an angular separation of 30 deg (BFC_{Rad} 30 deg $= 14.71 \pm 1.83$ mm and BFC_{Rad} 15 deg $= 15.39 \pm 1.64$ mm, $p = 0.010$). The two subjective exams, as it can be seen in Fig. 3, were more time consuming, but reducing the angular separation from 30 deg to 15 deg allowed a significant savings of almost half of the examination time (4:30 min when done in a 15 deg angular separation and 02:20 min when done in 30 deg). The same happened for the in-out routine, in which increasing the angular separation (maintaining the velocity of the peripheral stimulus) allowed us to significantly reduce the examination time (in-out 15 deg 15 $= 01:35$ min versus in-out

30 deg 15 = 00 : 51 min, $p < 0.001$; in-out 15 deg 25 = 01 : 20 min versus in-out 30 deg 25 = 00 : 46 min, $p < 0.001$).

4 Discussion

This is the third validation study conducted in apparatus intended to measure light distortion analysis. The previous one was published by Gutierrez et al.,[15] with the device Starlights published in the Journal of Biomedical Optics in 2003, and the other one was published by Meikies et al.[8] in 2014. More recently, different studies have used other methodologies without known validation studies.[9,10,12] Different from the previous devices, our system provides several metrics to characterize the size, shape, regularity, and location of the light distortion, while the previous devices concentrated only on the size of the photic phenomena.

With the present method we aim to overcome some of the limitations of previous methods.[3,4,8–10] Indeed, our results concerning the irregularity parameters show that the size of the distortion cannot be assumed as being rotationally symmetric. Further, while some previous devices have been validated considering different experimental setups,[15] others have used single setups without mentioning the potential variability under different experimental conditions.[8,10]

The present study shows that the examination of the light distortion size is consistent for different examination routines, on different days and is rapid. Factors such as the angular separation of the radial distances explored and speed of presentation of the stimuli have a minimal effect on the final outcomes. Increase in LDI and BFC_{Rad} with increasing central light intensity showed that the system is sensitive to changes in the source of glare by reflecting an increase in the size of the light distortion. However, its location, shape, and regularity represented by the parameters X_{Coord}, Y_{Coord}, BFC_{Orient}, BFC_{Irreg}, and $BFC_{IrregSD}$ did not change.

The first validation experiment of this study ascertained the influence of measuring the size and shape of the NVD with the patient's habitual correction and comparing it with the measurements when the vergence induce by the fixation target, that is a 2 m distance from the subject, is compensated. It can be seen that in terms of size of the measurements, there is no need to compensate the vergence induced by the fixation target once the size of the NVD between the two conditions is not statistically different and is strongly correlated. This might be expected if we consider the simulations presented in Fig. 4 for an average eye with a +0.3 microns Zernike SA and a pupil size of 6 mm for a nonaccommodating eye. While the positive defocus of −0.5 diopters (equivalent to defocus in the nonaccommodating eye at 2 m) would probably induce an increase in the size of the central light disturbance [Fig. 4(a)], full correction of such a defocus (using the +0.50 diopters lens in our experiment) would not change the apparent spread of light around the central spot of light [Fig. 4(c)] by much. In the present study, patients had their pupil dilated but were able to accommodate considering that all of them were young. Thus, we did not anticipate a difference between both conditions. With the +0.50 lens, the patient would be able to sharply see the central target without accommodation. Without the compensation lens, the patient would be required to accommodate approximately 0.50 D. This change could not change the subjective visualization of the central stimulus, or could even improve it by the reduction of the positive SA through accommodation.[16]

In the present sample, changing the pupil size from 3 to 6 mm did not have a significant impact on light distortion. This is an expected result considering that all subjects enrolled had moderate positive or neutral SA for a 6-mm pupil size. The role of the pupil in the optical quality is well known as the higher-order aberrations increase and as the pupil dilates. In fact, larger pupil sizes under photopic conditions are contra-indicative for some treatments such as orthokeratology or refractive corneal surgery because of the HOAs induced.[17] Despite this, the role of the pupil size as a main contributor to light disturbances is not so evident. Villa et al.[3] have found a moderate but not significant positive correlation between the pupil size and the magnitude of the light disturbances. This suggests that larger pupils are associated with stronger disturbances, but the pupil size by itself is not responsible for such effects. However, this could be the case for highly aberrated eyes, after refractive surgery, or orthokeratology,[17] but not in normal eyes with average values of SA as is the case in the present sample. Santolaria et al.[18] have recently measured the light distortion in patients undergoing corneal reshaping with contact lenses using the same experimental device used in the present study. They computed the corneal aberrations for different apertures of 3, 4.5, and 6 mm. they did not find significant correlations with the light distortion over a period of 1 month after treatment onset.[18] However, the pupil might also be relevant when studying light distortion induced by intraocular lenses with complex designs including diffractive apodized optics and multizone refractive optics.

The present device has been shown to be sensitive to differences in light distortion induced by IOL with different optical designs,[19] and multifocal contact lenses (unpublished results).

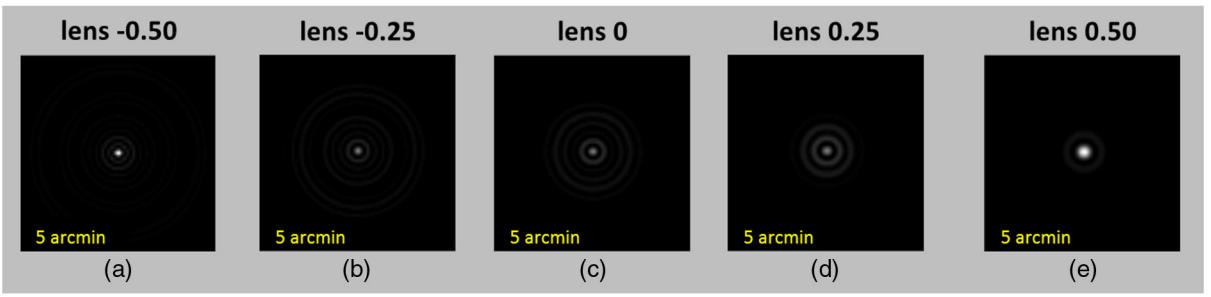

Fig. 4 (a) lens −0.5, (b) lens −0.25, (c) lens 0, (d) lens 0.25, and (e) lens 0.50. Simulations of the point spread function for 0.25 defocus steps in a theoretical eye with +0.3 microns of Zernike spherical aberration under nonaccommodation conditions. The situation where the vergence distance is not compensated is "lens −0.5" while the fully compensated situation for the 2 m (0.5 vergence) correspond the "lens 0" condition.

Another relevant result is the relationship between the intensity of the central source and the LDI. This trend could not be directly anticipated because the higher the brightness the more of a disturbance is usually reported by the patients, but this could be partially compensated by the miosis induced. Apparently, in this study, the increase in disturbance by the distribution of more light over a large area of the retina is not counterbalanced by the miosis that would be expected under such conditions. Pupil sizes measured for the central LED light at minimum, medium, and maximum intensities were 6.58 ± 0.08 mm, 5.11 ± 0.11 mm, and 4.44 ± 0.14 mm, respectively. This effect might be even more significant in elderly patients with a smaller dynamic range between natural pupil miosis and mydriasis.

The present method also has some limitations. The system uses detection stimuli rather than recognition stimuli such as letters or Landolt C's. This might allow the patient to provide a response even without recognizing the stimuli. This system prevents this effect by recording three different sets of measurements with stimuli presented in random order. When the patient provides false positive responses, the SD of the results in a given meridian will increase and the measure will be considered invalid. In the current setup, the system does not allow the identification of islands of negative dysphotopsia isolated from the center source of light. However, the aim of this device is to evaluate the light distortion surrounding a central source of light. Other methods, including automatic perimetry, can be used to define negative dysphotopsia.[6] Most of the previous methodologies reported do not provide information about the time spent in each measurement and the number of measurements used to obtain a single measurement. Both are relevant facts, as this method would probably involve examinations for elderly patients where attention and fatigue are potential issues. Our method allows obtaining a single measurement in less than 1 min per eye doing three repeated measures in this time.

As stated before, there are also several advantages of this instrument over the previous ones used for a similar purpose. First, being an entire physical device without intervention of video display units, cathodic ray tubes, flat screens or multimedia data-show projector, has the potential to have more consistency among examinations conducted in different settings. Second, the flexibility of setting different exam configurations might allow the expansion of the role of the system to different applications. Third, the different outcome metrics allow one to report the shape, regularity, and consistency of the results, and not only the average size of the light distortion assumed as a rotationally symmetric anomaly. This might no longer be the case in astigmatic defocus, comatic aberrations or corrective optical devices or surgical procedures including decentered optics.

The present study is limited by the fact all the subjects are young and healthy. Considering that postsurgical or diseased patients could present significantly higher values of light distortion, the results obtained in the present study cannot be directly extrapolated to those specific populations. For example, the examination time might increase as the light distortion increases. The difficulties found by older patients might be different from the ones found in the present sample. However, a recent study conducted in patients implanted with monofocal, bifocal and trifocal IOLs after cataract extraction demonstrated that the test is easily conducted in these clinical populations within an acceptable time period.[19]

In summary, the present study shows that the LDA might be a useful device in evaluating the light distortion, providing a comprehensive number of metrics to characterize the condition, and being robust to different sources of error in young healthy eyes. Specific clinical populations such as post-LASIK patients, postcorneal reshaping, and postcataract need to be addressed in future studies.

Acknowledgments

This study has been funded by the FEDER through the COMPETE Program and by the Portuguese Foundation for Science and Technology in the framework of projects PTDC/SAU-BEB/098391/2008, PTDC/SAU-BEB/098392/2008, and the Strategic Project PEST-C/FIS/UI607/2011.

Disclosure: The authors have a patent application related to the device described. The remaining authors declare that they do not have any proprietary or financial interest in any of the materials mentioned in this article.

References

1. N. I. Fan-Paul et al., "Night vision disturbances after corneal refractive surgery," *Surv. Ophthalmol.* **47**, 533–546 (2002).
2. B. Lackner et al., "Glare and halo phenomena after laser in situ keratomileusis," *J. Cataract Refractive Surg.* **29**, 444–450 (2003).
3. C. Villa et al., "Night vision disturbances after successful LASIK surgery," *Br. J. Ophthalmol.* **91**, 1031–1037 (2007).
4. S. Pieh et al., "Halo size under distance and near conditions in refractive multifocal intraocular lenses," *Br. J. Ophthalmol.* **85**, 816–821 (2001).
5. S. D. Klyce, "Night vision disturbances after refractive surgery: haloes are not just for angels," *Br. J. Ophthalmol.* **91**, 992–993 (2007).
6. J. T. Holladay, H. Zhao, and C. R. Reisin, "Negative dysphotopsia: the enigmatic penumbra," *J. Cataract Refractive Surg.* **38**, 1251–1265 (2012).
7. D. P. Pinero, D. Ortiz, and J. L. Alio, "Ocular scattering," *Optom. Vision Sci.* **87**, E682–E696 (2010).
8. D. Meikies et al., "Rostock glare perimeter: a distinctive method for quantification of glare," *Optom. Vision Sci.* **90**, 1143–1148 (2013).
9. M. C. Puell et al., "Normal values for the size of a halo produced by a glare source," *J. Refractive Surg.* **29**, 618–622 (2013).
10. A. L. Sheppard et al., "Visual outcomes and subjective experience after bilateral implantation of a new diffractive trifocal intraocular lens," *J. Cataract. Refractive Surg.* **39**, 343–349 (2013).
11. R. G. Anera et al., "Optical quality and visual discrimination capacity after myopic LASIK with a standard and aspheric ablation profile," *J. Refractive Surg.* **27**, 597–601 (2011).
12. J. J. Castro et al., "New testing software for quantifying discrimination capacity in subjects with ocular pathologies," *J. Biomed. Opt.* **16**, 015001 (2011).
13. J. M. M. Linhares et al., "Radiometric characterization of a novel LED array system for visual assessment," *J. Mod. Opt.* **60**, 1136–1144 (2013).
14. Y. H. Chan, "Biostatistics 104: correlational analysis," *Singapore. Med. J.* **44**(12), 614–619 (2003).
15. R. Gutierrez et al., "Simple device for quantifying the influence of halos after lasik surgery," *J. Biomed. Opt.* **8**, 663–667 (2003).
16. N. Lopez-Gil et al., "Shedding light on night myopia," *J. Vision* **12**, 4 (2012).
17. A. Queiros et al., "Effect of pupil size on corneal aberrations before and after standard laser in situ keratomileusis, custom laser in situ keratomileusis, and corneal refractive therapy," *Am. J. Ophthalmol.* **150**, 97–109 (2010).
18. E. Santolaria-Sanz et al., "Short-term changes in light distortion in orthokeratology subjects," *Biomed. Res. Int.* **2015**, 278425 (2015).
19. P. Brito et al., "Light distortion analysis as a possible indicator of visual quality after refractive lens exchange with AT LISA diffractive multifocal intraocular lenses," *J. Cataract Refractive Surg.* **41**, 613–622 (2015).

Helena Ferreira-Neves graduated in optometry and vision sciences in 2010 from the University of Minho and completed her master's degree in advanced optometry. Currently, she is a PhD student in the CEORLab. She has participated in several projects in the

areas of light distortion, presbyopia, and optical solutions for its compensation. She is the coauthor of articles published in scientific journals indexed in the ISI web of science and several communications in scientific conferences.

Rute Macedo-de-Araújo graduated in optometry and vision sciences from University of Minho. In 2014, she received her master's degree in advanced optometry. Currently, her research is focused on contact lenses, ocular surface, optical quality of the human eye, and light distortion. She has presented several communications in national and international congresses.

Laura Rico-del-Viejo received her bachelor's degree in optometry in 2012 at the University of Granada and is currently completing her master's degree in advanced clinical optometry at the University of Minho. Currently, her research is focused on light distortion, multifocal contact lenses, orthoqueratology, biomechanical properties of the cornea and contact lenses. She is the coauthor of one article published and has some papers submitted for publication.

Ana C. da-Silva graduated in optometry and vision sciences in 2010 from University of Minho and completed her master's degree in advanced optometry. She is the coauthor of articles published in different scientific journals indexed in the ISI web of science and several communications in national and international scientific conferences. Currently, she is in private practice.

António Queirós is an assistant professor in the University of Minho and course director of optometry and vision sciences. He received his PhD in 2011. He has published 42 articles in specialized journals and two chapters of books. He has participated in 19 events abroad and 24 in Portugal. He has received eight awards for presentation of papers at conferences.

José M. González-Méijome graduated in optics and optometry with honors from the University of Santiago de Compostela in 1997. He received his PhD in science at the University of Minho in 2007. Currently, he is an associate professor at the University of Minho and editor-in-chief of the Journal of Optometry: Peer-Reviewed Journal. He has authored 120 articles indexed in the ISI web of science with over 1200 citations, three books, and 15 book chapters.